J Membrane Biol (2013) 246:271–285
DOI 10.1007/s00232-013-9528-9

STIM1-Regulated Ca^{2+} Influx across the Apical and the Basolateral Membrane in Colonic Epithelium

Kaoru Onodera · Ervice Pouokam · Martin Diener

Received: 6 June 2012 / Accepted: 28 January 2013 / Published online: 9 February 2013

Abstract In nonexcitable cells, store-operated Ca^{2+} entry is the most important pathway for influx of extracellular Ca^{2+} serving as a second messenger in the cytoplasm. The present study investigated the expression, localization and polar distribution of two key components of store-operated Ca^{2+} entry identified, e.g., in lymphocytes or epithelial cell lines—STIM1 (stromal interacting molecule 1), working as a Ca^{2+} sensor in the endoplasmic reticulum, and Orai1, working as the (or part of the) store-operated Ca^{2+} channel in the plasma membrane—in a native intestinal epithelium, i.e., rat colon. Immunohistochemical investigations revealed expression of STIM1 and Orai1 in the rat colonic epithelium. Ca^{2+} store depletion led to a translocation of STIM1 both to the basolateral as well as to the apical cell pole as observed by confocal microscopy. A Ca^{2+} depletion/repletion protocol was used in Ussing chamber experiments to investigate the contribution of basolateral and apical store-operated Ca^{2+} entry to the induction of anion secretion. These experiments revealed that Ca^{2+}-dependent anion secretion was induced not only by basolateral Ca^{2+} repletion but also, to a lesser extent, by apical Ca^{2+} repletion. Both responses were suppressed by La^{3+}. The effect of basolateral Ca^{2+} repletion was significantly inhibited by brefeldin A, a blocker of vesicular transport from the endoplasmic reticulum to the Golgi apparatus. In a final series of experiments, fura-2-loaded HT29/B6 cells were used. A carbachol-induced increase in the cytosolic Ca^{2+} concentration was significantly reduced when cells were pretreated with siRNA against STIM1. In conclusion, these results demonstrate that STIM1 as a key component of intracellular Ca^{2+} signaling is expressed by rat colonic epithelium and is involved in the regulation not only of basolateral but also of apical Ca^{2+} influx.

Keywords Ca^{2+} · Cl^- secretion · HT29/B6 · Orai1 · Rat colon · STIM1

K. Onodera · E. Pouokam
Institute for Veterinary Physiology and Biochemistry, Justus-Liebig-University, Giessen, Germany

M. Diener (✉)
Institut für Veterinär-Physiologie und -Biochemie, Universität Gießen, Frankfurter Str. 100, Giessen, Germany
e-mail: Martin.Diener@vetmed.uni-giessen.de

Introduction

Changes in the cytosolic concentration of Ca^{2+} are one of the important signals which determine whether the colonic epithelium either absorbs water and electrolytes or secretes ions. This switching between absorption and secretion is controlled by neurotransmitters, hormones or paracrine substances usually acting via changes in the intracellular concentration of second messengers (Binder and Sandle 1994). Acetylcholine or its stable derivative carbachol, which are classical Ca^{2+}-dependent secretagogues, bind to G protein–coupled muscarinic receptors of types M_1 and M_3 at the basolateral side of the enterocytes (Haberberger et al. 2006). The consequence is the stimulation of a phospholipase C, which cleaves phosphatidylinositol-4,5-bisphosphate (PIP_2) into inositol-1,4,5-trisphosphate (IP_3), finally triggering the release of Ca^{2+} from Ca^{2+}-storing organelles such as the endoplasmic reticulum. This initial increase in the cytosolic Ca^{2+} concentration is followed in many cells by a capacitative Ca^{2+} influx via store-operated cation channels (Hoth and Penner 1992; Parekh and Penner 1997; Parekh 2006).

In recent years, the molecular identity of several key players involved in these processes has been discovered,

especially the family of stromal interacting molecule (STIM) proteins, which function as Ca^{2+} sensors in the endoplasmic reticulum, and the Orai proteins constituting the (or part of the) store-operated Ca^{2+} channel(s) in the plasma membrane (for review, see Taylor 2006; Hogan et al. 2010; Lee et al. 2010). STIM1 is a single-pass protein in the membrane of the endoplasmic reticulum. It possesses a Ca^{2+}-binding EF-hand domain near its N terminus, located in the lumen of the endoplasmic reticulum and serving as a Ca^{2+} sensor. In Jurkat cells, a human T-lymphocyte cell line, Ca^{2+} store depletion has been shown to induce the oligomerization and subsequent translocation of STIM1 into regions close to the plasma membrane. Here, it is trapped in so-called puncta by interaction with Orai (Wu et al. 2006; for review, see Hogan et al. 2010). The consequence is the activation of store-operated Ca^{2+}-permeable channels (Luik et al. 2006; Barr et al. 2008; Park et al. 2009; Lee et al. 2010).

Most data about the role of STIM1 have been obtained in nonpolarized cells such as lymphocytes (see, e.g., Wu et al. 2006; Barr et al. 2008) or nonconfluent HEK293 cells (see, e.g., Smyth et al. 2007; Wedel et al. 2007). Only a few studies have focused on the role of STIM1/Orai signaling in polarized epithelia such as the human colonic tumor cell line NCM460, where STIM1 also seems to be involved in the stimulation of cAMP production after emptying of intracellular Ca^{2+} stores (Lefkimmiatis et al. 2009); IEC-6 cells, a cell line from rat intestinal crypts, where STIM1 plays a role in wound healing (Rao et al. 2010); or pancreatic acinar cells (Petersen and Tepikin 2008; Hong et al. 2011).

In rat colonic epithelium, store depletion induced during whole-cell patch-clamp experiments by the use of a pipette solution (which replaces the cytosol during this type of experiment) with a high Ca^{2+}-buffering capacity activates a lanthanide-sensitive, nonselective cation conductance, which mediates capacitative Ca^{2+} influx after store depletion (Frings et al. 1999). Ussing chamber experiments suggest that in this epithelium not only a Ca^{2+} influx across the basolateral membrane is responsible for the regulation of the cytosolic Ca^{2+} concentration but also an influx across the apical membrane, which is necessary to activate Ca^{2+}-dependent K^+ (Schultheiss et al. 2003) or Cl^- channels (Schultheiss et al. 2005) in the apical membrane. Therefore, it seemed to be of interest to investigate the role of STIM1 and Orai1 in a native colonic epithelium with preserved polarity. Thus, the expression and migration of STIM1 in rat colonic epithelium was studied using conventional immunohistochemistry and confocal microscopy in Ca^{2+} depletion/repletion experiments in Ussing chambers combined with fura-2 and siRNA experiments in HT29/B6 cells, a human colonic tumor cell line.

Materials and Methods

Animals

For Ussing chamber and immunohistochemical experiments male and female Wistar rats with a body mass of 200–250 g were used. Animals were bred and housed at the Institute for Veterinary Physiology and Biochemistry of the Justus–Liebig–University Giessen (Giessen, Germany) at an ambient temperature of 22.5 °C and air humidity of 50–55 % on a 12:12 h light–dark cycle with free access to water and food until the time of the experiment. Experiments were approved by Regierungspräsidium Giessen (Giessen, Germany).

Solutions

The Ussing chamber and fura-2 experiments were performed using a Tyrode solution of the following composition (mmol l^{-1}): 140 NaCl, 5.4 KCl, 1.25 $CaCl_2$, 1 $MgCl_2$, 10 *N*-(2-hydroxyethyl)piperazine-*N*'-2-ethansulfonic acid (HEPES) and 12.2 glucose (pH 7.4), adjusted by NaOH/HCl. All HEPES-buffered solutions were gassed with O_2 in the Ussing chamber experiments. For morphometric analysis of STIM1 translocation, a CO_2/HCO_3^--buffered solution was used containing (mmol l^{-1}) 107 NaCl, 4.5 KCl, 25 $NaHCO_3$, 1.8 Na_2HPO_4, 0.2 NaH_2PO_4, 1.25 $CaCl_2$, 1 $MgSO_4$ and 12.2 glucose. The solution was gassed with 5 % (vol/vol) CO_2 and 95 % (vol/vol) O_2, at a temperature of 37 °C and pH of 7.4 (adjusted by $NaHCO_3$/HCl). For Ca^{2+}-free buffers, $CaCl_2$ was omitted in these buffer solutions without administration of a chelator. For immunohistochemical experiments, a 100 mmol l^{-1} phosphate buffer was used containing (mmol l^{-1}) 80 Na_2HPO_4 and 20 NaH_2PO_4; pH was 7.4 (adjusted by NaOH/HCl).

Cell Culture

HT29/B6 cells, a human colonic tumor cell line (Schmitz et al. 1999), were cultured on glass plates (diameter 13 mm) in 35-mm-diameter dishes. The culture medium (RPMI 1640; PAA, Cölbe, Germany) contained glutamine (2 mmol l^{-1}) and was enriched with 10 % (vol/vol) fetal calf serum. Culture was performed at 37 °C in a 95 % (vol/vol) air, 5 % (vol/vol) CO_2 atmosphere. Cells (3×10^5) were plated on the glass plates and cultured for 3–4 days.

Ussing Chamber Experiments

The serosa and muscularis propria were stripped away by hand to obtain a mucosa–submucosa preparation from the distal rat colon. Briefly, the colon was placed on a small plastic rod with a diameter of 5 mm. A circular incision

was made near the anal end with a blunt scalpel, and the serosa together with the muscularis propria were gently removed in a proximal direction.

The mucosa–submucosa preparation was fixed in a modified Ussing chamber bathed with a volume of 3.5 ml on each side of the mucosa. The tissue was incubated at 37 °C and short-circuited by a computer-controlled voltage-clamp device (Ingenieur Büro für Mess- und Datentechnik Mussler, Aachen, Germany) with correction for solution resistance. Tissue conductance (G_t) was measured every minute by the voltage deviation induced by a current pulse (±50 μA, duration 200 ms) under open-circuit conditions. Short-circuit current (I_{sc}) was continuously recorded on a chart recorder. I_{sc} is expressed as micro-equivalents per hour and square centimeter, i.e., the flux of a monovalent ion per time and area, with 1 μEq/(h cm^2) = 26.9 μA cm^{-2}.

Ca^{2+} Store Depletion

In order to study the effect of Ca^{2+} store depletion on the intracellular distribution of STIM1, mucosa–submucosa preparations were glued with tissue adhesive to plastic frames. Specimens were incubated at 37 °C for 2 h in a CO_2/HCO_3^--buffered solution either under control conditions (with Ca^{2+} in the buffer and in the absence of any drugs) or in Ca^{2+}-free buffer containing cyclopiazonic acid (10^{-5} mol l^{-1}). Then, the mucosa–submucosa preparation was cut from the frames and used for immunohistochemical staining (see below).

Imaging Experiments

For the fura-2 experiments, HT29/B6 cells grown on glass slides were used. They were incubated for 2 h with 6 μmol l^{-1} fura-2 acetoxymethyl ester (fura-2/AM; Life Technologies, Darmstadt, Germany). The dye ester not taken up by the cells was then washed away. Cells were superfused hydrostatically throughout the experiment with 140 mmol l^{-1} NaCl Tyrode. The perfusion rate was about 250 ml h^{-1}.

Changes in the cytosolic Ca^{2+} concentration were registered as changes in the fura-2 ratio (R; emission at an excitation wavelength of 340 nm divided by emission at an excitation wavelength of 380 nm). Experiments were carried out on an inverted microscope (Olympus IX-50) equipped with an epifluorescence setup and an image analysis system (Till Photonics, Martinsried, Germany). Emission above 470 nm was measured from the regions of interest, each of the size of about one cell. Data were sampled at 0.2 Hz. The baseline in the fluorescence ratio of the fura-2 signal was measured for several minutes before drugs were administered.

Immunohistochemical Experiments

The tissue was fixed overnight in phosphate buffer (100 mmol l^{-1}) containing 4 % (weight/vol) paraformaldehyde and embedded in gelatin (gelatin type A from porcine skin, 100 g · l^{-1}). The tissue was frozen in N_2-cooled isopentane; sections (6 μm thick) were cut and mounted on glass slides coated with gelatin containing chrome alaun (chromium[III] potassium sulfate, 0.5 g l^{-1}). For immunofluorescence staining, after rehydration in phosphate buffer, sections were incubated for 2 h in phosphate buffer containing 2 ml l^{-1} Triton X-100, 30 g l^{-1} bovine serum albumin and 100 ml l^{-1} goat serum (Chemicon, Temecula, CA), to block unspecific binding sites. The blocking solution was then removed, and sections were incubated with the primary antibody (see Table 1 for dilutions and sources) for 24 h at 4 °C. Each primary antibody was dissolved in phosphate buffer containing 1 ml l^{-1} Triton X-100, 5 g l^{-1} milk powder, 10 g l^{-1} bovine serum albumin and 10 ml l^{-1} goat serum. As a negative control some sections were incubated with a solution that did not contain the primary antibodies (see, e.g., Fig. 1, rows 2 and 4).

After rinsing with phosphate buffer, sections were incubated with the secondary antibody (see Table 1 for dilutions and sources) for 1 h at room temperature. After a further rinse with phosphate buffer, sections were incubated for 5 min with 3×10^{-7} mol l^{-1} 4′,6-diamidino-2-phenylindoldilactate (DAPI, Life Technologies). This dye was removed by washing the preparations four times for 5 min in phosphate buffer. Preparations were mounted on microscope slides using Hydromount™ (Biozym, Hessisch-Oldendorf, Germany), a nonfluorescing mounting medium. For staining of actin filaments, slides were incubated with phalloidin-FITC (4×10^{-7} mol l^{-1}; Sigma,

Table 1 Antibodies used

Target	Host species	Supplier	Final dilution
STIM1	Mouse (monoclonal)	Acris, Hildeshausen, Germany (AM03106PU-N)	1: 500
Orai1	Rabbit (polyclonal)	ProSci, Poway, CA (PSC-4281-C100)	1: 500
Mouse IgG	Goat	Cy3-coupled Dianova, Hamburg, Germany (115-165-003)	1: 500
Mouse IgG	Goat	Alexa 488-coupled, Life Technologies, Darmstadt, Germany (A11029)	1: 500
Rabbit IgG	Donkey	Cy3-coupled, Dianova, Hamburg, Germany (711-165-152)	1: 800

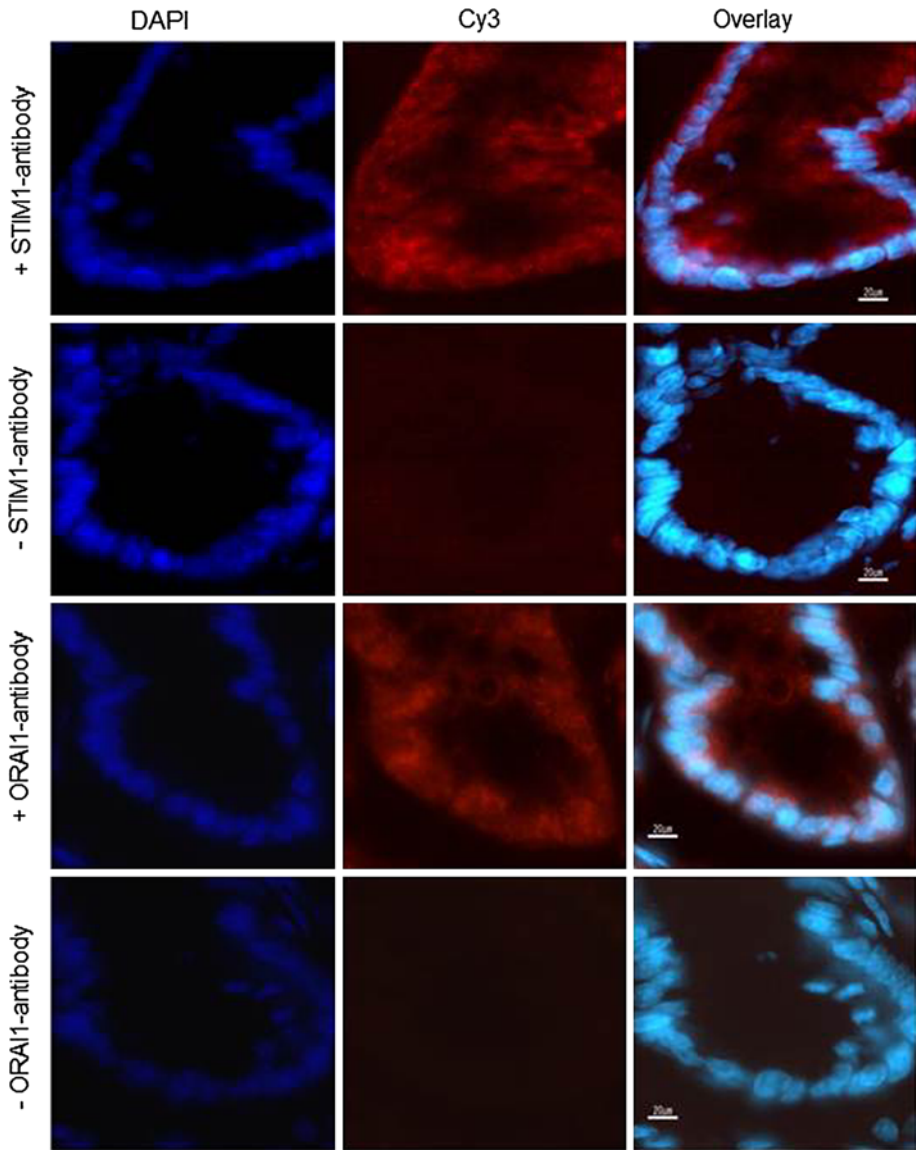

Fig. 1 Immunohistochemical detection of STIM1 (*row 1*) and Orai1 (*row 3*). Shown in each row is the fundus region of crypts in the rat colonic mucosa. *Left column* Nuclear staining with DAPI (*blue*), *middle column* immunohistochemical signal (Cy3-labeled, *red*), *right column* overlay of both. *Rows 1 and 3* Labeling. *Rows 2 and 4* Negative control without primary antibody against the respective protein. Scale bars (20 μm) are valid for all images. Typical results from three independent experiments (Color figure online)

Taufkirchen, Germany) for 36 h. Each immunohistochemical experiment was repeated at least three times with tissues from different animals.

Most preparations were examined on a fluorescence microscope (80i; Nikon, Düsseldorf, Germany). Digital images were taken with a black and white camera (DS-2 M B/Wc) using NIS Elements 2.30 software (all from Nikon) to adjust brightness, color and contrast. A part of each preparation was examined on a confocal microscope (DM LFSA; Leica, Wetzlar, Germany).

Morphometric Analysis

In order to quantify the distribution of STIM1 fluorescence along the longitudinal axis of epithelial cells, a line was drawn manually along the cell axis (see red line in Fig. 2 as example) using Leica confocal software. To describe the distribution of the STIM1 signal (*y* axis in Fig. 3), the total fluorescence intensity measured along this line was set as 100 %. In order to compensate for differences in the individual cell height, for the *x* axis the basal cell pole was set as 0 % and the apical cell pole as 100 % and the distribution of the STIM1 signal was plotted in 1 % steps along the drawn line (as indicated in the schematic drawing of Fig. 3). At the magnification used (63× objective), usually an average of 600 pixels were included in this measured line. Consequently, the gray-scale intensity of around five to seven pixels was averaged for each individual *x* value.

For the analysis of the putative downregulation of STIM1 by siRNA (see Fig. 9), randomly taken pictures from groups of HT29/B6 cells grown on glass slides were analyzed. All photographs were taken with the same setting (same exposure time and amplification) of the camera. An intensity value of 80 in the eight-bit gray-scale pictures

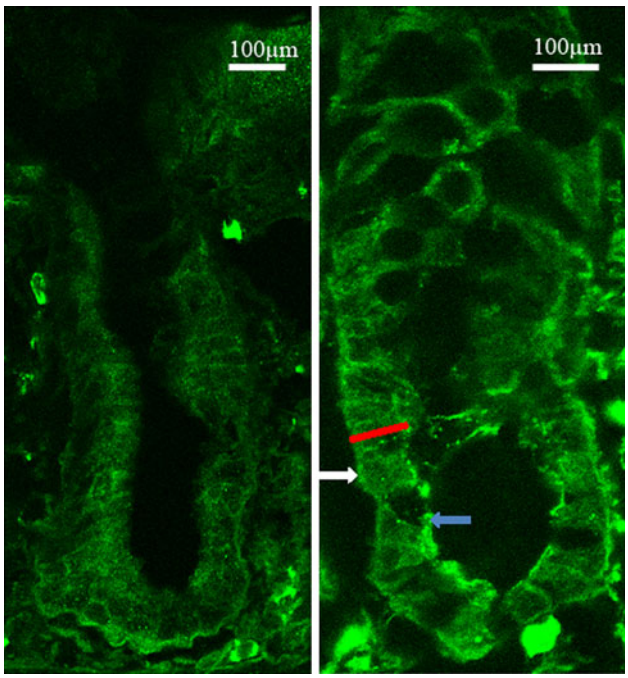

Fig. 2 Localization of STIM1 under control conditions (incubated for 2 h in CO_2/HCO_3^--buffered solution in the presence of extracellular Ca^{2+} without cyclopiazonic acid; *left*) and after store depletion (incubation for 2 h in Ca^{2+}-free, CO_2/HCO_3^--buffered solution containing 10^{-5} mol l^{-1} cyclopiazonic acid; *right*) observed with a confocal microscope. Basolateral (*white arrow*) and apical (*gray arrow*) cell poles are marked. *Red line* demonstrates how the distribution of STIM1 immunofluorescence was quantified along a line parallel to the longitudinal axis of a cell (see Fig. 3). Typical results from three independent experiments; for statistics, see Fig. 3 (Color figure online)

(corresponding to diffuse cellular background fluorescence) was set as threshold in order to discriminate between areas with and without cells on the filters. The mean gray-scale value in the cell-containing areas was then counted for each photograph taken from glass slides which had been treated with siRNA against STIM1 or control glass slides.

siRNA Experiments

For downregulation of STIM1, siRNA against STIM1 (sequence GGUGGUGUCUAUCGUUAUU; ABgene House, Epsom, UK) was used. Transfection was performed with Lipofectamine®. siRNA (final concentration 30 nmol l^{-1}) was dissolved in Lipofectamine (final concentration 60 µl l^{-1}) dissolved in Opti-MEM buffer (Life Technologies). Fifty microliters of this solution were pipetted into wells, which had been filled with 450 µl HT29/B6 cell suspension (cell density 10^5 ml^{-1}). For control experiments, a sham transfection without siRNA was performed. Cells were then cultured for 3–4 days.

Drugs

Forskolin was dissolved in ethanol (final maximal ethanol concentration 0.3 ml l^{-1}). Jasplakinolide (Life Technologies) was dissolved in methanol (final methanol concentration 2 ml l^{-1}). 2-APB, brefeldin A, cyclopiazonic acid (Alexis, Grünberg, Germany), cytochalasin D, phalloidin-FITC and thapsigargin (Calbiochem, Bad Soden, Germany) were dissolved in dimethyl sulfoxide (DMSO, final maximal concentration 2 ml l^{-1}). $CaCl_2$, carbachol, colchicine, $GdCl_3$, $LaCl_3$ and ruthenium red were dissolved in aqueous stock solutions. If not indicated differently, drugs were from Sigma.

Statistics

Results are given as mean ± standard error of the mean (SE) with the number (n) of investigated tissues or cells. For the comparison of two groups, either a Student's t test

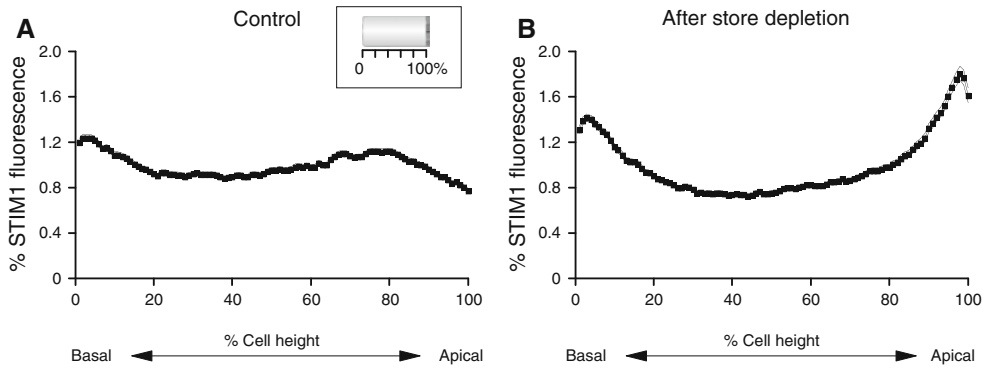

Fig. 3 Distribution of total STIM1 fluorescence measured along a line parallel to the longitudinal axis of epithelial cells (see *red line* in Fig. 2 as example). For the y axis, the total fluorescence along the longitudinal line was set as 100 %. In order to compensate for differences in individual cell height, for the x axis the basal cell pole was set as 0 % and the apical cell pole, as 100 % as indicated in the schematic drawing. Values are means ± SE, n = 220–240 cells

or a Mann–Whitney *U* test was applied. An *F* test decided which test method had to be used. Both paired and unpaired two-tailed Student's *t* tests were applied as appropriate. To compare more than two samples, an analysis of variance was performed followed by a post hoc Tukey's test. $P < 0.05$ was considered to be statistically significant.

Results

Basal Expression of STIM1 and Orai1

In order to find out whether rat colonic epithelial cells express the two key proteins involved in endoplasmic Ca^{2+}-sensing and capacitative Ca^{2+} entry involved in other cell types, STIM1 and Orai1, immunohistochemical experiments were performed with antibodies against both proteins. Immunoreactivity for STIM1 was found within the epithelial cells with no obvious gradient along the crypt–surface axis (Fig. 1, row 1; Fig. 2). A similar pattern was observed for Orai1 immunoreactivity (Fig. 1, row 3). The negative controls, in which the primary antibodies against the respective proteins had been omitted, did not reveal any signal (Fig. 1, rows 2 and 4).

Translocation of STIM1 after Store Depletion

In Jurkat cells, STIM1 is known to migrate to regions close to the plasma membrane after store depletion (Wu et al. 2006). In order to find out whether a similar translocation occurs in rat colonic epithelium and to study to which cell pole of the polarized epithelial cells STIM1 might migrate, the distribution of STIM1 was examined after Ca^{2+} store depletion by confocal microscopy. In order to induce Ca^{2+} store depletion, mucosa–submucosa preparations were incubated for 2 h in a Ca^{2+}-free solution in combination with cyclopiazonic acid (10^{-5} mol l^{-1}), a blocker of the sarcoplasmic–endoplasmic reticulum Ca^{2+}-ATPase (SERCA), to inhibit the SERCAs and to avoid the refilling of intracellular Ca^{2+} stores (Plenge-Tellechea et al. 1997). Control tissue was incubated for 2 h in Ca^{2+}-containing buffer solution without cyclopiazonic acid.

Under control conditions, the immunofluorescence of STIM1 was distributed more or less uniformly over the epithelial cells (Fig. 2, left). This changed dramatically after Ca^{2+} store depletion. Under these conditions, a condensation of the STIM1 immunofluorescence at the basal cell pole (marked with the white arrow in Fig. 2) and the lateral cell border was observed. This was not unexpected as the response to Ca^{2+}-dependent secretagogues is dependent on the presence of serosal Ca^{2+} (Zimmerman et al. 1983), which has led to the suggestion that intestinal epithelial cells regulate their cytosolic Ca^{2+} concentration mainly via basolaterally located Ca^{2+} channels/transporters. However, after store depletion, also a condensation of STIM1 immunofluorescence near the apical cell pole (marked with the gray arrow in Fig. 2) was observed.

In order to quantify this translocation, a morphometric analysis of the STIM1 immunofluorescence was performed. For this purpose, a line parallel to the longitudinal axis of individual epithelial cells was drawn (see red line in Fig. 2 as example). The total amount of fluorescence found along the longitudinal line was set as 100 %. Figure 3 describes the distribution of the STIM1 signal (as percent of the total fluorescence found along the line) along the longitudinal axis of the epithelial cells under control conditions and after store depletion. There was a clear increase in immunofluorescence near the basal and, even more pronounced, near the apical cell pole. In order to compensate for differences in individual cell height, for the *x* axis the basal cell pole was set as 0 % and the apical cell pole as 100 %, as indicated in the schematic drawing in Fig. 3. When the fluorescence in the five most basal compartments (0–5 % of cell height, i.e., the first five *x* values in Fig. 3) was integrated, the gray intensity increased in this compartment from 6.15 ± 0.14 ($n = 240$ cells) under control conditions to 6.90 ± 0.15 ($n = 220$ cells) after store depletion ($P < 0.05$). When the fluorescence in the five most apical compartments (95–100 % of cell height, i.e., the last five *x* values in the Fig. 3) was integrated, the gray intensity increased from 4.12 ± 0.08 ($n = 240$ cells) under control conditions to 8.64 ± 0.26 ($n = 220$ cells) after store depletion ($P < 0.05$).

As a further control to prove whether STIM1 translocated to regions near the cell membrane after store depletion, actin filaments, which form the terminal web below the brush border membrane, were costained using FITC-labeled phalloidin. Phalloidin staining resulted in a strong labeling of the apical cell region and the basolateral cell boundaries (Fig. 4, left). The simultaneous staining of STIM1 (Fig. 4, middle) and overlay of both signals (Fig. 4, right) clearly demonstrates that after store depletion STIM1 is found concentrated near both the basolateral as well as the apical cell borders.

Apical versus Basolateral Ca^{2+} Influx: Ussing Chamber Experiments

The translocation of STIM1, the presumed Ca^{2+} sensor of the endoplasmic reticulum, to both the basolateral as well as the apical cell pole suggests that store depletion might cause a Ca^{2+} influx across both the basolateral and apical membrane. In order to test this hypothesis, a Ca^{2+} depletion/repletion protocol was used in Ussing chamber experiments. An increase in the cytosolic Ca^{2+} concentration

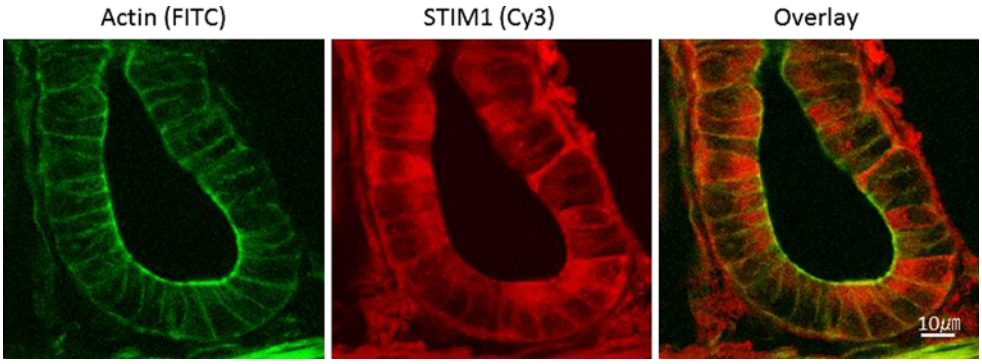

Fig. 4 Distribution of STIM1 immunofluorescence (labeled with Cy3 in *red*, *middle*) in relation to the distribution of actin filaments (labeled with FITC-coupled phalloidin, *left*) and overlay of both signals (*right*). Tissues had been incubated for 2 h in Ca^{2+}-free, CO_2/HCO_3^--buffered solution containing 10^{-5} mol · l^{-1} cyclopiazonic acid in order to induce Ca^{2+} store depletion. *Scale bar* (10 µm) is valid for all images. Typical results from three independent experiments (Color figure online)

is well known to activate Ca^{2+}-dependent K^+ channels (Böhme et al. 1991), which increases the driving force for Cl^- efflux across the dominant apical Cl^- channel, i.e., the cAMP-regulated cystic fibrosis transmembrane regulator (CFTR) channel. Consequently, the tissue was pretreated with the stimulator of adenylate cyclase(s) forskolin (5×10^{-6} mol l^{-1} at the mucosal and serosal sides) in order to activate CFTR channels via protein kinase A. The whole experiment was performed in the nominal absence of serosal Ca^{2+} to prevent Ca^{2+} influx from the extracellular space. After prestimulation of Cl^- secretion by forskolin, which induced an increase in I_{sc} of 3.94 ± 0.88 µEq/(h cm^2) ($n = 6$, Fig. 5a), Ca^{2+} stores were depleted by administration of the SERCA blocker thapsigargin (10^{-6} at the mucosal and serosal sides), which further increased I_{sc} by 0.33 ± 0.20 µEq/(h cm^2). When subsequently Ca^{2+} was readministered at the serosal side in a cumulative way, a transient and concentration-dependent increase in I_{sc} was observed, which reached a maximum at a Ca^{2+} concentration of 2.5–5 mmol l^{-1} (Fig. 5a). When a similar repletion protocol was run, in which Ca^{2+} was repleted from the mucosal side, the tissue proved to be less sensitive in comparison to serosal Ca^{2+}. A maximal increase in I_{sc} was observed at 10 mmol l^{-1}, and the increase in I_{sc} only amounted to about 25 % of the maximal increase observed with serosal Ca^{2+} (Fig. 5b), suggesting that only at a higher driving force (a higher concentration gradient) could an influx of mucosal Ca^{2+} induce anion secretion (see "Discussion").

Capacitative Ca^{2+} currents induced by Ca^{2+} store depletion in rat colonic epithelium are assumed to be mediated by lanthanide-sensitive, nonselective cation channels as shown by whole-cell patch-clamp experiments in isolated colonic crypts (Frings et al. 1999). Consequently, we tested whether the secretory response evoked by Ca^{2+} repletion was inhibited by La^{3+} (10^{-3} mol l^{-1} administered at either the serosal or the mucosal side). In order to evoke a roughly equieffective secretory response, Ca^{2+} concentrations of 1.25 and 12.5 mmol l^{-1} were selected for serosal and mucosal Ca^{2+} repletion, respectively. Serosal Ca^{2+} (1.25 mmol l^{-1}) caused an increase in I_{sc} of 2.10 ± 0.36 µEq/(h cm^2) ($n = 6$, Fig. 6a). However, when the tissue was pretreated with La^{3+} (10^{-3} mol l^{-1} at the serosal side), this increase only amounted to 0.19 ± 0.077 µEq/(h cm^2) ($n = 6$, $P < 0.05$ vs. response in the absence of La^{3+}; Fig. 6b). Serosal La^{3+} alone caused, after a paradoxical increase in I_{sc}, an inhibition of forskolin-induced I_{sc} (Fig. 6b). When the same protocol was used to characterize the effect of Ca^{2+} influx across the apical membrane, mucosal administration of Ca^{2+} (12.5 mmol l^{-1}) induced an increase in I_{sc} of 2.43 ± 1.73 µEq/(h cm^2) ($n = 6$, Fig. 6c). This secretory response was completely abolished when the tissue was pretreated with mucosal La^{3+} (10^{-3} mol l^{-1}, Fig. 6d). Under these conditions, Ca^{2+} even induced a small fall in I_{sc} of –0.27 ± 0.099 µEq/(h cm^2) ($n = 5$, $P < 0.05$ vs. response to Ca^{2+} in the absence of La^{3+}).

These experiments demonstrate that a La^{3+}-sensitive, capacitative Ca^{2+} entry also occurs from the apical side. However, its quantitative contribution is quite small compared to entry via the basolateral membrane. This conclusion is corroborated by the observation that it was not possible to induce a secretory response by Ca^{2+} repletion when the tissue was depleted of Ca^{2+} only at the mucosal side (data not shown).

Involvement of the Cytoskeleton

The question arises how the translocation of STIM1 to the basal and the apical epithelial cell poles is mediated. Ca^{2+} signaling, at least when induced by physiological agonists, needs an intact actin and microtubular cytoskeleton in 3T3 fibroblasts (Ribeiro et al. 1997). In the human embryonic kidney cell line HEK293 the Ca^{2+} release–activated

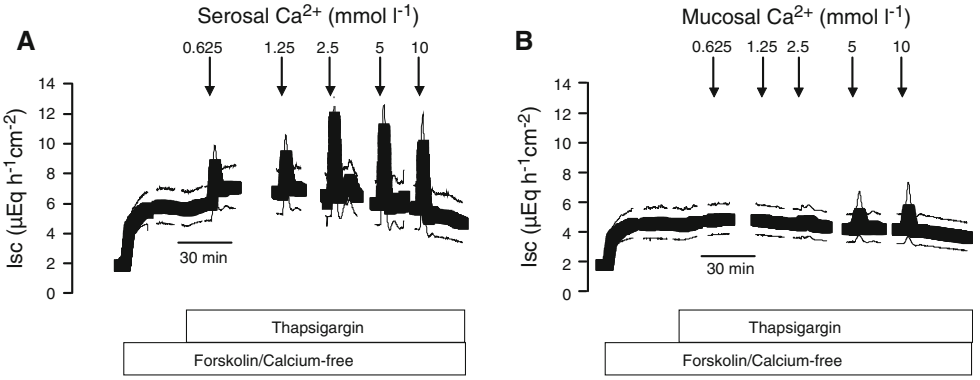

Fig. 5 Effects of Ca^{2+} depletion and cumulative repletion from either the serosal (**a**) or the mucosal (**b**) side of the epithelium. Chloride secretion was induced by forskolin (5×10^{-6} mol l^{-1} at the mucosal and serosal sides), and sarcoplasmic–endoplasmic Ca^{2+}-ATPase was inhibited by thapsigargin (10^{-6} mol l^{-1} at the mucosal and serosal sides). The whole experiment was performed in the nominal absence of serosal Ca^{2+}. Line interruptions are caused by omission of time intervals of 5–10 min in order to synchronize the tracings of individual records to the administration of drugs. Values are means (*symbols*) ± SEM (*lines*), $n = 6$

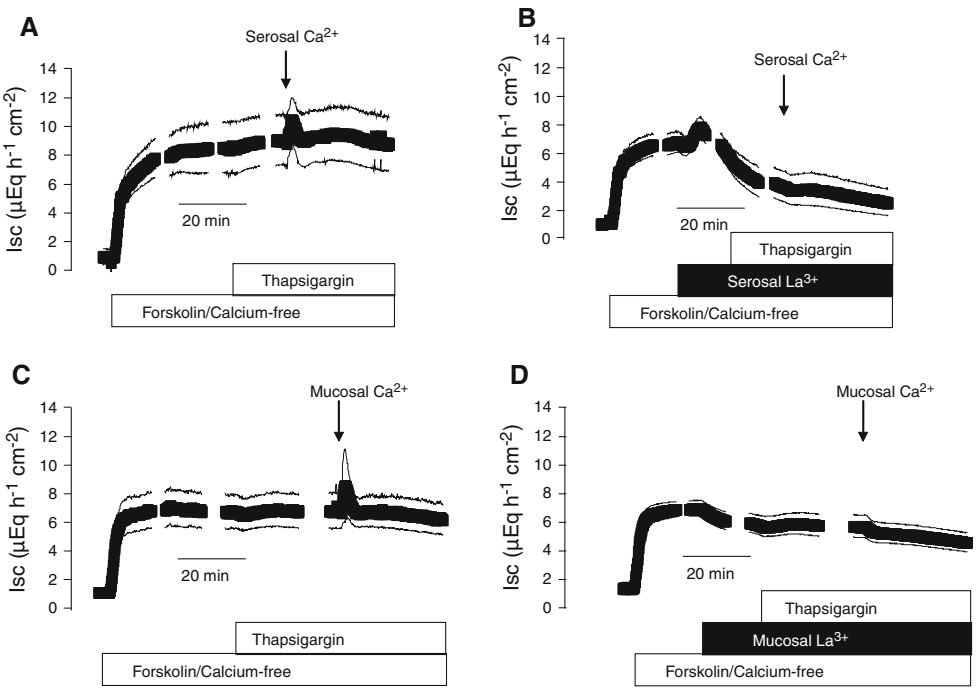

Fig. 6 Effects of Ca^{2+} depletion and repletion from either the serosal (**a, b**) or the mucosal (**c, d**) side of the epithelium. At the serosal side Ca^{2+} was repleted at a concentration of 1.25 mmol l^{-1}; at the mucosal side it was repleted at a concentration of 12.5 mmol l^{-1}. Chloride secretion was induced by forskolin (5×10^{-6} mol l^{-1} at the mucosal and serosal sides); sarcoplasmic–endoplasmic Ca^{2+}-ATPase was inhibited by thapsigargin (10^{-6} mol l^{-1} at the mucosal and serosal sides). The whole experiment was performed in the nominal absence of serosal Ca^{2+}. In the experiments depicted in **b** and **d**, $LaCl_3$ (10^{-3} mol l^{-1}, *black rectangle*) was added to the serosal or the mucosal compartment. Line interruptions are caused by omission of time intervals of 5–10 min in order to synchronize the tracings of individual records to the administration of drugs. Values are means (*symbols*) ± SEM (*lines*), $n = 5$–6. For statistics, see text

current (I_{CRAC}) is inhibited by nocodazole, a microtubule-depolymerizing drug (Smyth et al. 2007), and in Jurkat T lymphocytes colchicine interferes with intracellular STIM1 translocation (Barr et al. 2008). Consequently, it seemed to be of interest to study the effect of drugs that interfere with the cytoskeleton on basolateral or apical Ca^{2+} repletion. The Ca^{2+} depletion/repletion protocol was the same as depicted in Fig. 5 with the exception that the drugs interfering with the cytoskeleton were administered 30–45 min before administration of forskolin. All drugs were used in concentrations (and preincubation periods) which had been shown in previous experiments to interfere with swelling-induced K^+ efflux (Ribeiro et al. 2001) or Ca^{2+}-induced Cl^- efflux (Hennig et al. 2008) at rat colonic mucosa

without destroying the integrity of the epithelium, which is a prerequisite for transepithelial voltage clamping in the Ussing chamber.

Colchicine (2.5×10^{-5} mol l^{-1} at the serosal side), a drug inducing the depolymerization of microtubuli (Schroer and Sheetz 1990), inhibited neither the increase in I_{sc} evoked by basolateral nor that evoked by apical Ca^{2+} repletion (Table 2). For unknown reasons, the increase in I_{sc} induced by apical Ca^{2+} was unusually large, both in the absence (6.15 ± 1.41 μEq/[h cm^2]) and in the presence (7.81 ± 3.73 μEq/[h cm^2]) of colchicine in these series of experiments.

Pretreatment of the tissue with jasplakinolide (10^{-6} mol l^{-1} at the serosal side), which strengthens the actin cytoskeleton by stabilization of F-actin (Ahmed et al. 2000; Bubb et al. 2000), did not inhibit the I_{sc} evoked by basolateral Ca^{2+} repletion. There was a tendency for a reduction of the I_{sc} induced by apical Ca^{2+} repletion, which was, however, not statistically significant (Table 2). Unfortunately, it was not possible to test the effect of depolymerization of F-actin as pretreatment with cytochalasin D (10^{-5} mol l^{-1} at the serosal side) induced a very strong increase in tissue conductance, suggesting a disturbance of the integrity of the epithelium (data not shown).

Finally, the ability of brefeldin A (2×10^{-5} mol l^{-1} at the serosal side), which inhibits vesicular transport from the endoplasmic reticulum to the Golgi apparatus (Misumi et al. 1986; Klausner et al. 1992), to interfere with the secretory response evoked by Ca^{2+} repletion was tested. Brefeldin A reduced the increase in I_{sc} evoked by basolateral Ca^{2+} by about two-thirds from 8.89 ± 0.97 μEq/(h cm^2) ($n = 5$) under control conditions to 3.20 ± 1.00 μEq/(h cm^2) in the presence of brefeldin A ($n = 5$, $P < 0.05$). Apparently, the response evoked by apical Ca^{2+} repletion was reduced from 2.56 ± 1.62 μEq/(h cm^2) ($n = 6$) to 0.56 ± 0.34 μEq/(h cm^2) ($n = 5$), although this effect did not reach statistical significance due to the large variability of the response.

Ca^{2+}-Imaging Experiments with HT29/B6 Cells

As there are no pharmacological inhibitors available to interfere with the function of STIM1, an siRNA approach was used to investigate how inhibition of STIM1 activity via downregulation might interfere with agonist-induced Ca^{2+} signaling. Because long-term preincubation with the respective siRNA is a prerequisite for this maneuver, these experiments were performed with a colonic tumor cell line, HT29/B6, using the stable acetylcholine derivative carbachol as agonist.

In order to verify the presence of store-operated Ca^{2+} entry in HT29/B6 cells, a Ca^{2+} depletion/repletion protocol was used. Intracellular Ca^{2+} stores were depleted by incubation in a nominal Ca^{2+}-free extracellular medium combined with the SERCA blocker cyclopiazonic acid (10^{-5} mol l^{-1}). Readministration of Ca^{2+} (1.25 mmol l^{-1}) under these conditions evoked a prompt increase in the fura-2 signal ratio by 0.16 ± 0.010 ($n = 82$, Fig. 7a). When cells were pretreated with Gd^{3+} (5×10^{-6} mol l^{-1}), this increase was reduced to 0.066 ± 0.0091 ($n = 54$, $P < 0.05$ vs. response in the absence of Gd^{3+}, Fig. 7b). 2-APB (10^{-5} mol l^{-1}), which, in addition to its inhibitory effect on IP_3 receptors, is known to block some types of store-operated Ca^{2+} channels (Diver et al. 2001), did not inhibit the Ca^{2+} influx after store depletion as the increase in the fura-2 ratio amounted to 0.31 ± 0.016 ($n = 41$) under control conditions and 0.49 ± 0.015 ($n = 93$) in the presence of 2-APB.

Carbachol (5×10^{-5} mol l^{-1}) evoked a prompt increase in the fura-2 ratio signal, i.e., an increase in the cytosolic Ca^{2+} concentration, in these cells (Fig. 8a). Within 1 min, the fura-2 ratio signal rose to a maximum

Table 2 Ca^{2+}-induced I_{sc} after Ca^{2+} depletion

Conditions	Peak by basolateral Ca^{2+} ΔI_{sc} (μEq/[h cm^2])	n	Peak by apical Ca^{2+} ΔI_{sc} (μEq/[h cm^2])	n
Without colchicine	7.73 ± 0.51	7	6.15 ± 1.41	6
With colchicine	6.28 ± 0.32	7	7.81 ± 3.73	6
Without jasplakinolide	5.39 ± 0.99	6	1.32 ± 0.40	9
With jasplakinolide	4.35 ± 0.99	6	0.72 ± 0.25	9
Without brefeldin A	8.89 ± 0.97	5	2.56 ± 1.62	6
With brefeldin A	3.20 ± 1.00*	5	0.56 ± 0.34	5

Effect of basolateral Ca^{2+} repletion (1.25 mmol l^{-1} $CaCl_2$ at the serosal side) or apical Ca^{2+} repletion (12.5 mmol l^{-1} $CaCl_2$ at the mucosal side) after serosal Ca^{2+} depletion (140 NaCl/O Ca^{2+}/1 Mg^{2+} Tyrode at the serosal side). Tissues were incubated in a Ca^{2+}-free Tyrode solution, prestimulated with forskolin (5×10^{-6} mol l^{-1} at the mucosal and serosal sides) and thapsigargin (10^{-6} mol l^{-1} at the mucosal and serosal sides). If present, colchicine (2.5×10^{-5} mol l^{-1} at the serosal side), jasplakinolide (10^{-6} mol l^{-1} at the serosal side) or brefeldin A (2×10^{-5} mol l^{-1} at the serosal side) were administered 30–45 min before the administration of forskolin. Values are means ± SE and are given as difference from baseline just prior to administration of Ca^{2+}

*$P < 0.05$ vs. Ca^{2+}-induced I_{sc} in the absence of the respective inhibitor

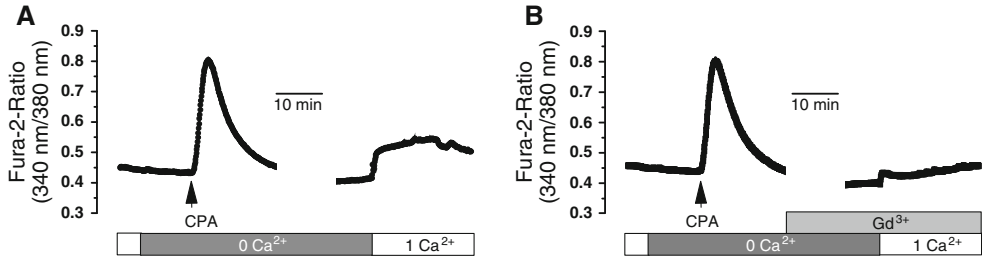

Fig. 7 Effect of Ca^{2+} store repletion after Ca^{2+} store depletion via incubation in a Ca^{2+}-free medium (*dark gray rectangle*, 0 Ca^{2+}) combined with cyclopiazonic acid (*CPA*; *arrow*, 10^{-5} mol l^{-1}) in the absence (**a**) and presence (**b**) of Gd^{3+} (*light gray rectangle*, 5×10^{-6} mol l^{-1}). The concentration of Ca^{2+} used for Ca^{2+} repletion (*white rectangles*) amounted to 1.25 mmol l^{-1}. Line interruptions served to synchronize individual recordings to Ca^{2+} readministration. The fura-2 signal ratio is given as means (*symbols*) ± SEM (*parallel continuous lines*), $n = 52$–84. For statistics, see text

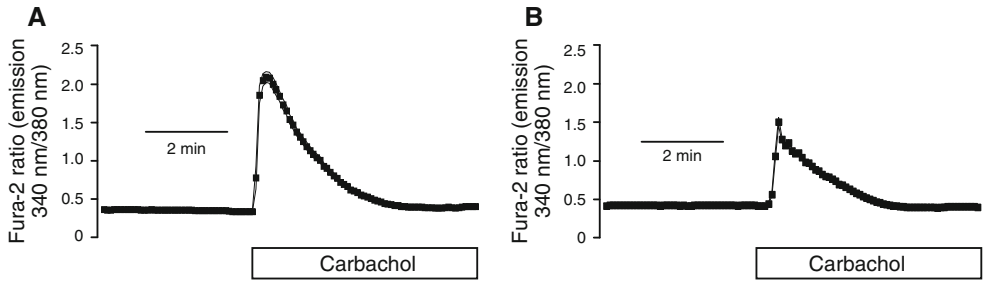

Fig. 8 Increase in the cytosolic Ca^{2+} concentration as revealed by the increase in the fura-2 signal ratio induced by carbachol (5×10^{-5} mol l^{-1}, *white rectangle*) under control conditions (**a**) or after transfection of cells with siRNA against STIM1 (**b**). Data are means (*symbols*) ± SE (*lines*), $n = 27$–65. For statistics, see Table 3

(peak) and then declined exponentially. In order to quantify this second phase of the carbachol response, the increase in the fura-2 ratio above the former baseline was measured 5 min after administration of the cholinergic agonist. Typically, the carbachol response is assumed to represent an initial Ca^{2+} release via stimulation of IP_3 receptors followed by an influx of extracellular Ca^{2+} (Parekh and Penner 1997). Indeed, when internal Ca^{2+} stores were depleted by prior administration of the SERCA blocker cyclopiazonic acid (10^{-5} mol l^{-1}), the effect of carbachol was nearly suppressed (Table 3). The peak of the carbachol response, but not the 5-min value, was significantly reduced in the presence of 2-APB (10^{-5} mol l^{-1}), a blocker of IP_3 receptors (Maruyama et al. 1997), whereas ruthenium red (5×10^{-5} mol l^{-1}), which inhibits ryanodine receptors (Xu et al. 1999), was ineffective (Table 3), confirming the involvement of IP_3 receptors in the response to the cholinergic agonist in this cell line.

In accordance with the general model, preincubation in a nominal Ca^{2+}-free buffer reduced significantly the second phase of the carbachol response (i.e., the value measured 5 min after administration of carbachol) by about 50 %. However, also the peak value induced by carbachol, which is assumed to represent a Ca^{2+} release from internal stores, was reduced significantly, which might suggest a partial depletion of intracellular Ca^{2+} stores in the absence of extracellular Ca^{2+} (Table 3). Surprisingly, La^{3+} (10^{-3} mol l^{-1}), which has been shown to block capacitative Ca^{2+} currents in rat colonic epithelium (Frings et al. 1999) as well as in HT29 cells (Kerst et al. 1995), had a quite paradoxical effect: it induced a transient series of Ca^{2+} spikes in the majority of cells (not shown) and inhibited the peak response but not the long-lasting increase in the fura-2 ratio signal induced by carbachol (Table 3, see "Discussion").

When cells were pretreated with the siRNA against STIM1, two significant changes were observed in the response evoked by carbachol. The peak increase in the cytosolic Ca^{2+} concentration was reduced by about 40 %, and 5 min after administration of the cholinergic agonist, the increase in cytosolic Ca^{2+} concentration was totally abolished (Fig. 8, Table 3).

Immunohistochemichal Staining of HT29/B6 Cells

In order to prove the downregulation of STIM1 expression by the siRNA protocol used, immunohistochemical staining against STIM1 was performed, which revealed a pronounced reduction of STIM1 immunoreactivity in cells transfected with siRNA compared to nontransfected cells (Fig. 9). To quantify this downregulation, a morphometric analysis was performed. When analyzing the intensity value of the STIM1 signal in cell-containing areas of the

Table 3 Carbachol-induced Ca^{2+} signals in HT29/B6 cells

	ΔFura-2 ratio evoked by carbachol		
Conditions	Peak	5 min	*n*
Without cyclopiazonic acid	0.97 ± 0.070	0.26 ± 0.026	84
With cyclopiazonic acid	0.005 ± 0.006*	−0.075 ± 0.009*	84
Without 2-APB	1.65 ± 0.091	0.65 ± 0.043	72
With 2-APB	1.15 ± 0.065*	0.54 ± 0.041	72
Without ruthenium red	1.67 ± 0.11	0.33 ± 0.036	72
With ruthenium red	1.55 ± 0.083	0.48 ± 0.041	77
With Ca_e^{2+}	1.20 ± 0.065	0.35 ± 0.029	72
No Ca_e^{2+}	0.84 ± 0.059*	0.16 ± 0.022*	60
Without $LaCl_3$	1.14 ± 0.066	0.10 ± 0.018	84
With $LaCl_3$	0.50 ± 0.057*	0.21 ± 0.032*	81
Without siRNA	1.88 ± 0.064	0.027 ± 0.011	27
With siRNA	1.13 ± 0.039*	–0.027 ± 0.004*	65

Effect of carbachol (5×10^{-5} mol l^{-1}) on the fura-2 ratio signal in HT29/B6 cells. The response was tested in the absence or presence of cyclopiazonic acid (10^{-5} mol l^{-1}), 2-aminoethoxydiphenyl borate (2-APB, 10^{-5} mol l^{-1}), ruthenium red (5×10^{-5} mol l^{-1}) or La^{3+} (10^{-3} mol l^{-1}) after transfection of cells with siRNA against STIM1 or in the presence and absence of extracellular Ca^{2+} (Ca_e^{2+}). Data are given as difference from baseline just prior to administration of carbachol (Δfura-2 ratio). The maximum fura-2 ratio reached within 5 min (peak) and the value 5 min after administration of carbachol are given. Values are means ± SE

*$P < 0.05$ vs. response to carbachol in the absence of the respective inhibitor

individual photographs (each taken with the same camera setting), the mean gray-scale value in the cell-containing areas was reduced from 144.7 ± 3.6 ($n = 46$ photos) under control conditions to 115.4 ± 3.1 ($n = 48$) after siRNA treatment ($P < 0.05$ vs. control).

Discussion

The present results demonstrate that STIM1 and Orai1, two key proteins involved in store-operated Ca^{2+} signaling known from other cell types (for reviews, see, e.g., Taylor 2006; Hogan et al. 2010; Lee et al. 2010), are expressed by rat colonic epithelium (Fig. 1). STIM1 is in general thought to be activated by Ca^{2+} store depletion via its EF-hand domain located in the lumen of the endoplasmic reticulum (Stathopulos et al. 2008), followed by oligomerization and accumulation in puncta near the plasma membrane (Wu et al. 2006), where it interacts with Ca^{2+}-permeable channels that mediate the influx of extracellular Ca^{2+} into the cytosol. Such a translocation of STIM1 after store depletion was observed also in rat colonic epithelium (Figs. 2, 3). Interestingly, an accumulation of STIM1 was found not only near the basolateral membrane (quantified in Fig. 3 as an increase in STIM1 immunoreactivity close to the basal cell pole) but also near the apical membrane of these polarized cells.

In general, influx of Ca^{2+} from the serosal compartment, i.e., via the basolateral membrane, is thought to be involved in anion secretion induced by typical Ca^{2+}-dependent secretagogues, such as carbachol, as removal of serosal Ca^{2+} strongly inhibits (but does not abolish) carbachol-induced Cl^- secretion (Zimmerman et al. 1983). The increase in the cytosolic Ca^{2+} concentration leads to the activation of Ca^{2+}-dependent K^+ channels (Böhme et al. 1991), increasing the driving force for Cl^- efflux across apical Cl^- channels. However, studies in which the basolateral membrane was bypassed due to incubation in a high-K^+ buffer (i.e., basolateral depolarization) clearly revealed that the activation of apical Ca^{2+}-dependent K^+

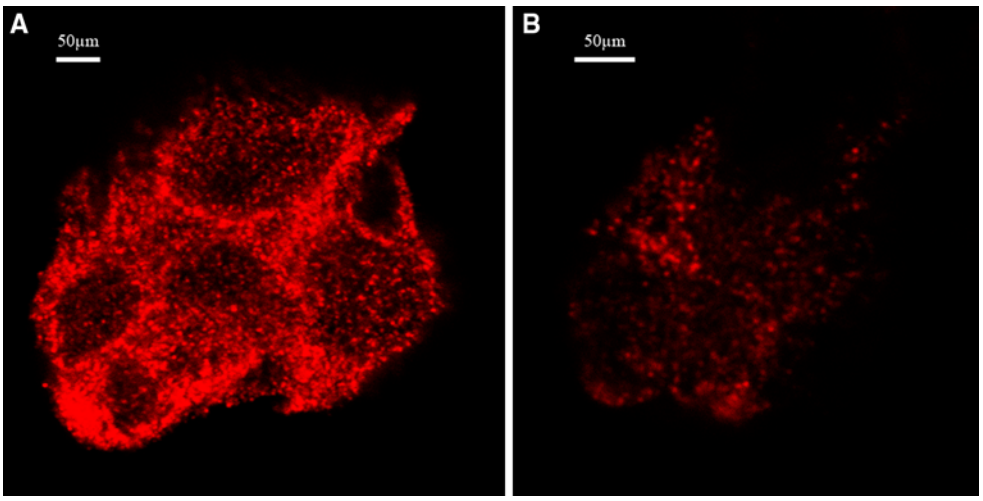

Fig. 9 Immunohistochemichal staining of HT29 cells grown on glass plates under control conditions (**a**) and after transfection with siRNA against STIM1 (**b**). All photographs were taken with the same exposure time of the camera. Representative pictures from three independent experiments. For statistics of the morphometric analysis, see text (Color figure online)

channels, from which several types such as the large-conductance $K_{Ca1.1}$ (Sorensen et al. 2010) or the intermediate-conductance $K_{Ca3.1}$ (Kumar et al. 2010) are expressed in colonic epithelia, is dependent on the presence of mucosal Ca^{2+} (Schultheiss et al. 2003). Also, stimulation of the Ca^{2+}-dependent apical Cl^- conductance in the same tissue depends on the presence of mucosal, but not serosal, Ca^{2+} (Schultheiss et al. 2005).

The present results clearly demonstrate that store depletion by SERCA blockade combined with the absence of serosal Ca^{2+} activates a Ca^{2+} influx across both the basolateral as well as the apical membrane when using the I_{sc} induced by Ca^{2+} repletion as read-out. In accordance with the classical view of the overwhelming effect of serosal Ca^{2+}, serosal Ca^{2+} proved to be more efficient and more potent at inducing secretion in this Ca^{2+} depletion/repletion protocol compared to mucosal Ca^{2+} (Fig. 5).

The ability of Ca^{2+} readministration to evoke anion secretion, which leads to the measured increase in I_{sc} (Fig. 5), might not only depend on the amount of Ca^{2+} entry via store-operated Ca^{2+} channels but also be modified by Ca^{2+}-sensing receptors. These are found on both the apical and the basolateral membrane and inhibit intestinal fluid and ion secretion via modulation of cyclic nucleotide degradation (Geibel et al. 2006). Thus, a different activity of these G protein–coupled receptors might contribute to the different effectiveness of mucosal and serosal Ca^{2+} repletion. A further possibility, which must be considered, is the possibility that, especially in the presence of high mucosal Ca^{2+} concentrations, there might be some diffusion of Ca^{2+} via the tight junctions into the serosal medium, which might allow Ca^{2+} influx via basolateral store-operated Ca^{2+} channels. However, the response to mucosal Ca^{2+} repletion was suppressed by mucosal La^{3+} (Fig. 6d), for which tight junctions are normally impermeable (see, e.g., Böhme et al. 1992). This, together with the observation that in basolaterally depolarized epithelia serosal Ca^{2+} is ineffective and only mucosal Ca^{2+} is able to stimulate a Ca^{2+}-dependent apical Cl^- conductance (Schultheiss et al. 2005), strongly argues that an influx of mucosal Ca^{2+} via the apical membrane is indeed involved in the regulation of colonic ion transport.

The molecular nature of the cation-permeable pathway in the apical or the basolateral membrane of rat colonic epithelium is yet unclear. Orai1, which constitutes the (or part of the) Ca^{2+}-permeable store-operated ion channel in other cell types, e.g., lymphocytes (for review, see Hogan et al. 2010), is found at both cell poles (Fig. 1) and could, therefore, contribute to forming the Ca^{2+} influx pathway activated by store depletion. However, also cation channels of the transient receptor potential channel (TRPC) family are reported to contribute to the molecular identity of store-operated cation channels in a human salivary gland cell line (Parvez, et al. 2008) or human embryonic kidney (HEK293) cells (Liao et al. 2007; Alicia et al. 2008), although in some studies no contribution of TRPC channels could be observed (DeHaven et al. 2009).

Both the secretory responses evoked by Ca^{2+} store depletion after basolateral and after apical Ca^{2+} repletion were suppressed by La^{3+}, which blocks the nonselective cation conductance induced by store depletion in whole-cell patch-clamp experiments at isolated rat colonic crypts (Frings et al. 1999) or HT29 cells (Kerst et al. 1995). This would fit the assumption that an electrogenic Ca^{2+} influx via cation channels might be activated by translocation of the Ca^{2+} sensor STIM1. However, the Ca^{2+} channel protein Orai1, which is thought to interact with STIM1, is also associated with an Na^+–Ca^{2+} exchanger as after knockdown of STIM1 with siRNA expression of the Na^+–Ca^{2+} exchanger NCX1 was reduced in human aortic myocytes (Baryshnikov et al. 2009). Na^+–Ca^{2+} exchangers, when running in the reverse mode, e.g., after membrane depolarization, can also work as Ca^{2+}-loading transporters; and at least in the apical membrane of rat colonic epithelium, NCX1 has been demonstrated immunohistochemically (Schultheiss et al. 2003).

A prerequisite for store-operated Ca^{2+} signaling via the STIM1/Orai signaling pathway is the translocation of STIM1 in the form of oligomers close to the plasma membrane (for review, see Taylor 2006; Hogan et al. 2010; Lee et al. 2010), a phenomenon which was also observed for native intestinal epithelium in the present study (Figs. 2, 3). This translocation has been studied in detail in HEK293 cells, where STIM1, which had been tagged with yellow fluorescent protein, colocalized with α-tubulin. Furthermore, nocodazole, a microtubule-depolymerizing drug, inhibited I_{CRAC}, which is carried by highly selective Ca^{2+} channels with a low single-channel conductance, although the process of STIM1 translocation is not thought to be directly mediated by microtubules (Smyth et al. 2007). In 3T3 fibroblasts, the increase in the cytosolic Ca^{2+} concentration induced by agonists coupled to IP_3-mediated Ca^{2+} release induced by stimulation of G protein–coupled receptors leading to phospholipase C activation, but not that induced by SERCA blockade with thapsigargin, was abolished by disruption both of the microtubular cytoskeleton with nocodazole and of the actin cytoskeleton with cytochalasin D (Ribeiro et al. 1997), whereas in smooth muscle cells from guinea pig the disruption of the actin cytoskeleton enhanced capacitative Ca^{2+} entry (Morales et al. 2005). In rat colonic epithelium, however, preincubation with colchicine did not affect the secretory response evoked by basolateral or apical Ca^{2+} repletion. Also, stabilization of F-actin with jasplakinolide did not inhibit the I_{sc} evoked by Ca^{2+} repletion (Table 2). However, brefeldin, a drug which inhibits the anterograde

transport of vesicles from the endoplasmic reticulum to the Golgi apparatus and promotes at the same time the reverse transport (Misumi et al. 1986; Klausner et al. 1992), significantly inhibited the response to basolateral Ca^{2+} repletion and reduced (although not significantly due to the in general higher variability of the response evoked by apical Ca^{2+} repletion) the effect of apical Ca^{2+} readministration (Table 2). Thus, a transport step between both cellular organelles seems to be involved in the I_{sc} response evoked by Ca^{2+} depletion/repletion.

Knockdown of STIM1 by siRNA has been used successfully as a tool to demonstrate the involvement of STIM1 in Ca^{2+} signaling, e.g., in HEK293 cells (Alicia et al. 2008) or vascular smooth muscle cells from rats (Lu et al. 2009) or mice (Ng et al. 2010). A similar approach was used to prove the involvement of STIM1 in receptor-induced Ca^{2+} signaling in the colonic tumor cell line HT29. In accordance with the general model that stimulation of basolateral muscarinic receptors leads to the IP_3-mediated release of Ca^{2+} from internal stores followed by a store-operated Ca^{2+} entry, the increase in the cytosolic Ca^{2+} concentration was abolished by prior store depletion with cyclopiazonic acid, whereas 2-APB, which blocks IP_3 receptors, only inhibited the early phase of the carbachol response (Table 3). There was, however, also a striking difference from the general model when considering the effect of La^{3+}. Although in HT29 cells Ca^{2+} store depletion (via increasing the Ca^{2+} buffer capacity of the whole-cell pipette solution) has been shown to activate a lanthanide-sensitive cation current (Kerst et al. 1995), La^{3+} only inhibited the early phase, i.e., the peak of the increase in the cytosolic Ca^{2+} concentration. However, La^{3+} did not inhibit but, rather, enhanced the late phase of the carbachol response (quantified 5 min after administration of the cholinergic agonist in Table 3). The reason for this paradoxical effect is unknown, but La^{3+} has been shown to activate Ca^{2+}-permeable cation channels of the type TRPC5 via an increase in the channel open probability (Jung et al. 2003). In contrast, in native rat colonic epithelium, where Ca^{2+} store depletion evokes a similar lanthanide-sensitive cation current as observed in HT29 cells (Frings et al. 1999), La^{3+} suppressed the effect of basolateral as well as apical Ca^{2+} store depletion (Fig. 6). This may either indicate nonspecific effects of La^{3+}, e.g., on Ca^{2+}-extruding transporters, or suggest differences in Ca^{2+} signaling after "strong" store depletion with Ca^{2+}-free extracellular medium combined with SERCA blockade compared to the more physiological receptor-mediated stimulation of Ca^{2+} signaling. Indeed, such differences have been observed in 3T3 cells, where Ca^{2+} signaling induced by agonists is suppressed by drugs that interfere with the actin or the microtubular cytoskeleton, whereas Ca^{2+} signals induced by thapsigargin or injection of IP_3 were resistant against these drugs (Ribeiro et al. 1997). A plausible explanation for these differences may be that G protein–coupled receptors, which activate phospholipase C, simultaneously alter the content of the plasma membrane in PIP_2, the precursor of IP_3, which has been shown to interfere with Ca^{2+} channels in intestinal epithelial cells from *Caenorhabditis elegans* (Xing and Strange 2010). Nevertheless, preincubation with siRNA against STIM1 both downregulated STIM1 protein expression (Fig. 9) as well as shortened the carbachol-induced increase in the cytosolic Ca^{2+} concentration, as had to be expected when considering the presumed role of STIM1 as a Ca^{2+} sensor in the endoplasmic reticulum (Table 3).

In conclusion, the present results demonstrate that one of the key proteins involved in Ca^{2+} signaling in nonexcitable cells, STIM1, is also involved in Ca^{2+} signaling in a native intestinal epithelium, i.e., rat colon, where it translocates to the plasma membrane after store depletion in order to evoke a Ca^{2+} influx predominantly across the basolateral membrane supported by an influx of Ca^{2+} across the apical membrane. Differences in the kinetics of Ca^{2+} signals in the apical and basal cytosol are well known from pancreatic acinar cells, one of the best-characterized polarized cell types regarding Ca^{2+} signaling, where agonist-induced rises in the cytosolic Ca^{2+} concentration develop faster at the apical cell pole (for review, Petersen and Tepikin 2008). Here, even gradients in the distribution of STIM1 along the lateral membrane with a concentration near the tight junctions and differential distribution of Orai and TRPC channels, with which STIM1 is thought to interact to activate Ca^{2+}-permeable channels for store-operated Ca^{2+} entry, have been observed (Hong et al. 2011). The present results indicate that, at least in colonic epithelium, even the apical membrane can contribute to Ca^{2+} signaling, although the pore-forming proteins which finally mediate Ca^{2+} influx into the cell across both membranes still have to be determined.

Acknowledgement This work was supported by the Deutsche Forschungsgemeinschaft, grant Di 388/11-1

References

Ahmed N, Ramjeesingh M, Wong S, Varga A, Garami E, Bear CE (2000) Chloride channel activity of CIC-2 is modified by the actin cytoskeleton. Biochem J 352:789–794

Alicia S, Angelica Z, Carlos S, Alfonso S, Vaca L (2008) STIM1 converts TRPC1 from a receptor-operated to a store-operated channel: moving TRPC1 in and out of lipid rafts. Cell Calcium 44:479–491

Barr VA, Bernot KM, Srikanth S, Gwack Y, Balagopalan L, Regan CK, Helman DJ, Sommers CL, Oh-hora M, Rao A, Samelson LE (2008) Dynamic movement of the calcium sensor STIM1 and the calcium channel Orai1 in activated T-cells: puncta and distal caps. Mol Biol Cell 19:2802–2817

Baryshnikov SG, Pulina MV, Zulian A, Linde CI, Golovina VA (2009) Orai1, a critical component of store-operated Ca^{2+} entry, is functionally associated with Na^{+}/Ca^{2+} exchanger and plasma membrane Ca^{2+} pump in proliferating human arterial myocytes. Am J Physiol Cell Physiol 297:C1103–C1112

Binder HJ, Sandle GI (1994) Electrolyte transport in the mammalian colon. In: Johnson LR (ed) Physiology of the gastrointestinal tract. Raven Press, New York, pp 2133–2171

Böhme M, Diener M, Rummel W (1991) Calcium- and cyclic AMP–mediated secretory responses in isolated colonic crypts. Pfluegers Arch 419:144–151

Böhme M, Diener M, Mestres P, Rummel W (1992) Direct and indirect actions of $HgCl_2$ and methyl mercury chloride on the permeability and chloride secretion of the rat colonic mucosa. Toxicol Appl Pharmacol 114:285–294

Bubb MR, Spector I, Beyer BB, Fosen KM (2000) Effects of jasplakinolide on the kinetics of actin polymerization. An explanation for certain in vivo observations. J Biol Chem 275: 5163–5170

DeHaven WI, Jones BF, Petranka JG, Smyth JT, Tomita T, Bird GS, Putney JW Jr (2009) TRPC channels function independently of STIM1 and Orai1. J Physiol 587:2275–2298

Diver JM, Sage SO, Rosado JA (2001) The inositol trisphosphate receptor antagonist 2-aminoethoxydiphenylborate (2-APB) blocks Ca^{2+} entry channels in human platelets: cautions for its use in studying Ca^{2+} influx. Cell Calcium 30:323–329

Frings M, Schultheiß G, Diener M (1999) Electrogenic Ca^{2+} entry in the rat colonic epithelium. Pfluegers Arch 439:39–48

Geibel J, Sritharan K, Geibel R, Geibel P, Persing JS, Seeger A, Roepke TK, Deichstetter M, Prinz C, Cheng SX, Martin D, Hebert SC (2006) Calcium-sensing receptor abrogates secretagogue-induced increases in intestinal net fluid secretion by enhancing cyclic nucleotide destruction. Proc Natl Acad Sci USA 103:9390–9397

Haberberger R, Schultheiss G, Diener M (2006) Epithelial muscarinic M_1 receptors contribute to carbachol-induced ion secretion in mouse colon. Eur J Pharmacol 530:229–233

Hennig B, Schultheiss G, Kunzelmann K, Diener M (2008) Ca^{2+}-induced Cl^{-} efflux at rat distal colonic epithelium. J Membr Biol 221:61–72

Hogan PG, Lewis RS, Rao A (2010) Molecular basis of calcium signaling in lymphocytes: STIM and ORAI. Annu Rev Immunol 28:491–533

Hong JH, Li Q, Kim MS, Shin DM, Feske S, Birnbaumer L, Cheng KT, Ambudkar IS, Muallem S (2011) Polarized but differential localization and recruitment of STIM1, Orai1 and TRPC channels in secretory cells. Traffic 12:232–245

Hoth M, Penner R (1992) Depletion of intracellular calcium stores activates a calcium current in mast cells. Nature 355:353–356

Jung S, Mühle A, Schaefer M, Strotmann R, Schultz G, Plant TD (2003) Lanthanides potentiate TRPC5 currents by an action at extracellular sites close to the pore mouth. J Biol Chem 278:3562–3571

Kerst G, Fischer KG, Normann C, Kramer A, Leipziger J, Greger R (1995) Ca^{2+} influx induced by store release and cytosolic Ca^{2+} chelation in HT29 colonic carcinoma cells. Pfluegers Arch 430:653–665

Klausner RD, Donaldson JG, Lippincott-Schwartz J (1992) Brefeldin A: insights into the control of membrane traffic and organelle structure. J Cell Biol 116:1071–1080

Kumar NSN, Singh SK, Rajendran VM (2010) Mucosal potassium efflux mediated via Kcnn4 channels provides the driving force for electrogenic anion secretion in colon. Am J Physiol Gastrointest Liver Physiol 299:G707–G714

Lee KP, Yuan JP, Hong JH, So I, Worley PF, Muallem S (2010) An endoplasmic reticulum/plasma membrane junction: STIM1/Orai1/TRPCs. FEBS Lett 584:2022–2027

Lefkimmiatis K, Srikanthan M, Maiellaro I, Moyer MP, Curci S, Hofer AM (2009) Store-operated cyclic AMP signalling mediated by STIM1. Nat Cell Biol 11:433–442

Liao Y, Erxleben C, Yildirim E, Abramowitz J, Armstrong DL, Birnbaumer L (2007) Orai proteins interact with TRPC channels and confer responsiveness to store depletion. Proc Natl Acad Sci USA 104:4682–4687

Lu WJ, Wang J, Peng GY, Shimoda LA, Sylvester JT (2009) Knockdown of stromal interaction molecule 1 attenuates store-operated Ca^{2+} entry and Ca^{2+} responses to acute hypoxia in pulmonary arterial smooth muscle. Am J Physiol Lung Cell Mol Physiol 297:L17–L25

Luik RM, Wu MM, Buchanan J, Lewis RS (2006) The elementary unit of store-operated Ca^{2+} entry: local activation of CRAC channels by STIM1 at ER-plasma membrane junctions. J Cell Biol 174:815–825

Maruyama T, Kanaji T, Nakade S, Kanno T, Mikoshiba M (1997) 2-APB, 2-aminoethoxydiphenyl borate, a membrane-penetrable modulator of $Ins(1,4,5)P_3$-induced Ca^{2+} release. J Biochem 122: 498–505

Misumi Y, Misumi Y, Miki K, Takatsuki A, Tamura G, Ikehara Y (1986) Novel blockade by brefeldin A of intracellular transport of secretory proteins in cultured rat hepatocytes. J Biol Chem 261:11398–11403

Morales S, Camello PJ, Rosado JA, Mawe GM, Pozo MJ (2005) Disruption of actin filamentous actin cytoskeleton is necessary for the activation of capacitative calcium entry in native smooth muscle cells. Cell Signal 17:635–645

Ng CL, Ramduny D, Airey JA, Singer CA, Keller PS, Shen XM, Tian H, Valencik M, Hume JR (2010) Orai1 interacts with STIM1 and mediates capacitative Ca^{2+} entry in mouse pulmonary arterial smooth muscle cells. Am J Physiol Cell Physiol 299:C1079–C1090

Parekh AB (2006) On the activation mechanism of store-operated calcium channels. Pfluegers Arch 453:303–311

Parekh AB, Penner R (1997) Store depletion and calcium influx. Physiol Rev 77:901–930

Park CY, Hoover PJ, Mullins FM, Bachhawat P, Covington ED, Raunser S, Walz T, Garcia KC, Dolmetsch RE, Lewis RS (2009) STIM1 clusters and activates CRAC channels via direct binding of a cytosolic domain to Orai1. Cell 136:876–890

Parvez S, Beck A, Peinelt C, Soboloff J, Lis A, Monteilh-Zoller M, Gill DL, Fleig A, Penner R (2008) STIM2 protein mediates distinct store-dependent and store-independent modes of CRAC channel activation. FASEB J 22:752–761

Petersen OH, Tepikin AV (2008) Polarized calcium signaling in exocrine gland cells. Annu Rev Physiol 70:273–299

Plenge-Tellechea F, Soler F, Fernadez-Belda F (1997) On the inhibition mechanism of sarcoplasmic or endoplasmic reticulum Ca^{2+}-ATPases by cyclopiazonic acid. J Biol Chem 272: 2794–2800

Rao JN, Rathor N, Zou TT, Liu L, Xiao L, Yu TX, Cui YH, Wang JY (2010) STIM1 translocation to the plasma membrane enhances intestinal epithelial restitution by inducing TRPC1-mediated Ca^{2+} signaling after wounding. Am J Physiol Cell Physiol 299: C579–C588

Ribeiro CMP, Reece J, Putney JW Jr (1997) Role of the cytoskeleton in calcium signaling in NIH 3T3 cells. An intact cytoskeleton is required for agonist-induced $[Ca^{2+}]_i$ signaling, but not for capacitative calcium entry. J Biol Chem 272:26555–26561

Ribeiro R, Heinke B, Diener M (2001) Cell volume–induced changes in K^{+} transport across the rat colon. Acta Physiol Scand 171:445–458

Schmitz H, Fromm M, Bentzel CJ, Scholz P, Detjen K, Mankertz J, Bode H, Epple HJ, Riecken EO, Schulzke JD (1999) Tumor necrosis factor-alpha (TNF alpha) regulates the epithelial barrier

in the human intestinal cell line HT-29/B6. J Cell Sci 112:137–146

Schroer TA, Sheetz MP (1990) Functions of microtubule-based motors. Annu Rev Physiol 53:629–652

Schultheiss G, Ribeiro R, Schäfer KH, Diener M (2003) Activation of apical K^+-conductances by muscarinic receptor stimulation in rat distal colon: fast and slow components. J Membr Biol 195:183–196

Schultheiss G, Siefjediers A, Diener M (2005) Muscarinic receptor stimulation activates a Ca^{2+}-dependent Cl^- conductance in rat distal colon. J Membr Biol 204:117–127

Smyth JT, DeHaven WI, Bird GS, Putney JW Jr (2007) Role of the microtubule cytoskeleton in the function of the store-operated Ca^{2+} channel activator STIM1. J Cell Sci 120:3762–3771

Sorensen MV, Matos JE, Praetorius HA, Leipziger J (2010) Colonic potassium handling. Pfluegers Arch 459:645–656

Stathopulos PB, Zheng L, Li GY, Plevin MJ, Ikura M (2008) Structural and mechanistic insights into STIM1-mediated initiation of store-operated calcium entry. Cell 135:110–122

Taylor CW (2006) Store-operated Ca^{2+} entry: a STIMulating stOrai. Trends Biochem Sci 31:597–601

Wedel B, Boyles RR, Putney JW Jr, Bird GS (2007) Role of the store-operated calcium entry proteins STIM1 and Orai1 in muscarinic cholinergic receptor–stimulated calcium oscillations in human embryonic kidney cells. J Physiol 579:679–689

Wu MM, Buchanan JA, Luik RM, Lewis RS (2006) Ca^{2+} store depletion causes STIM1 to accumulate in ER regions closely associated with the plasma membrane. J Cell Biol 174:803–813

Xing J, Strange K (2010) Phosphatidylinositol 4,5-bisphosphate and loss of PLCγ activity inhibit TRPM channels required for oscillatory Ca^{2+} signaling. Am J Physiol Cell Physiol 298:C274–C282

Xu L, Tripathy A, Pasek DA, Meissner G (1999) Ruthenium red modifies the cardiac and skeletal muscle Ca^{2+} release channels (ryanodine receptors) by multiple mechanisms. J Biol Chem 274:32680–32691

Zimmerman TW, Dobbin JW, Binder HJ (1983) Role of calcium in the regulation of colonic secretion in the rat. Am J Physiol 244:G552–G560